Fluorinated Benzyloxyphenyl Piperidine-4-carboxamides with Dual Function against Thrombosis: Inhibitors of Factor Xa and Platelet Aggregation

Modesto de Candia,[†] Francesco Liantonio,[†] Andrea Carotti,[†,§] Raimondo De Cristofaro,[‡] and Cosimo Altomare*[,†]

Dipartimento Farmaco-chimico, University of Bari, Via Orabona 4, I-70125, Bari, Italy, Hemostasis Research Centre, Institute of Internal Medicine and Geriatrics, Catholic University School of Medicine, Largo F. Vito 1, I-00168 Rome, Italy

Received September 12, 2008

A series of benzyloxy anilides of nipecotic (**5**, **6**) and isonipecotic (**7**, **8**) acids were synthesized and assayed in vitro as inhibitors of ADP-induced platelet aggregation and the blood coagulation enzymes factor Xa (FXa) and thrombin (FIIa). An exploration of effects of the amidine group attached at the piperidine nitrogen, position and substitution (F, phenyl) of the benzyloxy group, and addition of fluorine/s on the second (distal) phenyl ring, led us to single out some promising isonipecotamide derivatives **7**. Addition of *meta*-F and *para*-CF_3 on the distal phenyl ring resulted in a 6-to-18-fold enhancement of the FXa potency and in 2-to-4-fold increase of the antiplatelet potency, the last depending to a large extent upon lipophilicity. Two congeners of *N*-{[3-(1,1′-biphenyl-4-yl)methoxy]phenyl}piperidine-4-carboxamide (**7m** and **7p**) proved to be potent FXa-selective inhibitors (K_i = 130 and 57 nM, respectively) and antiplatelet agents and were identified as leads for developing new dual function antithrombotic drugs.

Introduction

Thrombotic events are leading causes of cardiovascular-associated death in the developed world.[1,2] Prophylaxis and treatment of arterial thrombosis in patients with cardiovascular diseases (e.g., atherosclerotic vascular disease, acute coronary syndrome (ACS[a]) including myocardial infarctions and unstable angina) are achieved using antiplatelet drugs,[3] whereas venous thrombosis (e.g., deep vein thrombosis (DVT) and pulmonary embolism (PE)) is treated with anticoagulant drugs, which inhibit various proteases in the blood coagulation cascade.[4−6]

Platelets are primary components of hemostasis,[7] but their activation is involved in the pathogenesis of thromboembolic diseases[8] and complications following percutaneous coronary intervention.[9] They can be activated by a number of agonists such as adenosine 5′-diphosphate (ADP), thromboxane A_2 (TxA_2), thrombin, platelet activating factor (PAF), epinephrine (EPN), and collagen.[10] Antiplatelet drugs include the most commonly used aspirin, the thienopyridine derivative clopidogrel, and its more powerful analogue prasugrel, which are antagonists of the cell-surface ADP receptor $P2Y_{12}$,[11] the $\alpha_2\beta_3$-integrin antagonists (also known as glycoprotein IIb/IIIa-GpIIa/IIIb-receptor antagonists), such as the specific antibody abciximab, the oligopeptide eptifibatide and nonpeptide inhibitor tirofiban,[12] and the recently discovered antagonists of the thrombin receptor PAR-1 (protease-activated receptor-1) such as SCH 530348 undergoing phase-III clinical trials.[13]

Anticoagulant therapy, used to treat a variety of conditions including cure and prevention of venous thromboembolism (VTE) and long-term prevention of ischemic stroke in patients with atrial fibrillation, involves heparins and the vitamin K antagonist warfarin.

The main side effect of most of the available antithrombotic drugs is bleeding, whereas therapy of insufficient intensity (aspirin, clopidogrel) can entail a risk of recurrent thrombosis. A number of drug-class-specific adverse reactions include, for instance, aspirin-related gastrointestinal ulcers and bleeding, thrombotic thrombocytopenic purpura that may be associated to thienopyridines,[14] heparin-induced thrombocytopenia (reduced with low-molecular weight heparins),[15] warfarin-induced skin necrosis.[16] Moreover, warfarin has a narrow therapeutic window, and its activity is affected by diet and genetic makeup, so requiring continuous monitoring for accurate dosing.[17] For all these reasons, the search for new antiplatelet and anticoagulant drugs, with better therapeutic windows and easier-to-use than the existing ones, still represents a challenging goal.[5,18]

Among the novel antithrombotics in development, several orally administered direct inhibitors of thrombin (FIIa)[19] and factor Xa (FXa)[20] offer the promise of better activities and lesser side effects. Two notable examples are the thrombin inhibitor dabigatran etexilate,[21] which is as effective as enoxaparin at reducing the risk of VTE,[22] and the FXa-selective inhibitor rivaroxaban,[23] which has shown a favorable safety/efficacy balance for preventing VTE after major orthopedic surgery.[24] The coagulation enzyme FXa has been recognized as a promising target for the development of new antithrombotic drugs. FXa inhibitors seemed to have a lower risk of bleeding than heparin and warfarin.[25] Indeed, they do not block thrombin directly but decrease the amplified generation of thrombin, allowing the existing levels of thrombin to ensure primary hemostasis.[26]

The combined use of antiplatelet and anticoagulant agents showed additional benefits over anticoagulants alone in patients with prosthetic hearth valves,[27] as well as in patients with atrial fibrillation.[28] Furthermore, old and recent literature showed that VTE and arterial disease share common risk factors.[29] Although

* To whom correspondence should be addressed. Phone: +39-080-5442781. Fax: +39-080-5442230. E-mail: altomare@farmchim.uniba.it.

† Dipartimento Farmaco-chimico, University of Bari.

‡ Hemostasis Research Centre, Catholic University School of Medicine.

§ Present address: Dipartimento di Chimica e Tecnologia del Farmaco, University of Perugia, Via del Liceo 1, I-06123 Perugia, Italy.

[a] Abbreviations: ACS, acute coronary syndrome; ADP, adenosine 5′-diphosphate; aPTT, activated partial tromboplastin time; α-CT, α-chymotrypsin; DAG, 1,2-diacylglycerol; DVT, deep vein thrombosis; EPN, epinephrine; FIIa, thrombin; FXa, factor Xa; GpIIb/IIIa, glycoprotein IIb/IIIa; IP_3, inositol 1,4,5-triphosphate; PAF, platelet activating factor; PAR-1, protease-activated receptor-1; PE, pulmonary embolism; PLs, phospholipids; PRP, platelet-rich plasma; PPP, platelet-poor plasma; TxA_2, thromboxane A_2; VTE, venous thromboembolism.

10.1021/jm801141f CCC: $40.75
Published on Web 02/04/2009

Chart 1. Progression and Design of Nipecotamide-Based Composite Antithrombotics

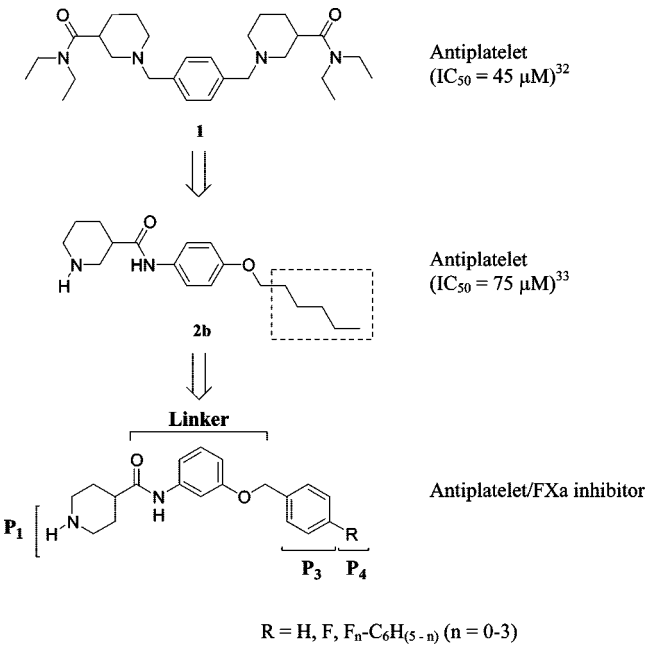

numerous investigations suggest the existence of an association between VTE and atherosclerosis, the nature of this relation has not been clarified. It seems, however, that VTE, promoting inflammatory processes, could exert a causative role in the pathogenesis of atherothrombosis. Indeed, there are many examples of conditions accounting for both arterial and venous thromboembolic disorders, such as antiphospholipid antibodies, hyperhomocysteinemia, factor V Leiden or prothrombin gene mutation, high levels of factor VIII:C, myeloproliferative disorders, and HIV infection.

Even though the appropriateness of a combined anticoagulant and antiplatelet therapy for patients with multiple disorders is still discussed,[30] compounds combining in the same molecule anticoagulant and platelet antiaggregatory activities are believed to be promising drugs. Compared to a combination of antiplatelet and anticoagulant drugs, a single composite (dual function) agent should be advantageous, thanks to an expected less complex pharmacokinetics, a likely lower incidence of side effects, and less demanding clinical studies.[31]

In our ongoing research addressed toward new antithrombotic agents endowed with dual antithrombotic function, we used as a suitable scaffold for design piperidine-3(or 4)-carboxylic acid phenyl amide. In previous studies by Gollamudi et al.,[32] derivatives of piperidine-3-carboxamide, such as the bis-nipecotamide derivatives **1** (Chart 1), proved to be inhibitors of platelet aggregation in vitro and in vivo. From a mechanistic point of view, type **1** compounds showed ability to penetrate the platelet membranes and to interact with anionic phospholipids (PLs), mainly phosphatidylinositides, decreasing their turnover, release of second messengers (i.e., inositol 1,4,5-triphosphate IP_3 and 1,2-diacylglycerol DAG), intracellular calcium levels, and consequently inhibiting platelet activation and aggregation. A few years ago, we also have reported a large series of nipecotamides, among which *N*-[4-(hexyloxy)phenyl]piperidine-3-carboxamide (**2b**) proved to be in vitro inhibitor of human platelet aggregation induced by ADP, arachidonic acid, and EPN, with a potency comparable to that of **1** (Chart 1), and demonstrated the impact of lipophilicity on their antiplatelet activity by a parabolic relationship between inhibition data (IC_{50}) and log *P*-related parameters.[33]

In this work, we synthesized other anilide derivatives of nipecotic and isonipecotic acid, replacing in particular the *n*-hexyloxy groups in the para position with R-substituted benzyloxy ones, our investigation pursuing a 2-fold goal: (i) to improve the antiplatelet activity of this series and (ii) to further modify the structure of the most promising antiplatelet candidate, used as a scaffold, for building up compounds, which additionally can attain FXa inhibition. Thus, we initially replaced the chiral nipecotic with the achiral isonipecotic acid, then shifted the substitution position of the benzyl group on the −HN-C_6H_4−O− linker from the para to meta position, and finally attempted to improve binding of the P_1 and P_4 groups into the "arginine recognition pocket" S_1 and "aryl binding site" S_3/S_4 of FXa, respectively.

Our early binding models, based on docking calculation (QXP software[34]) between the designed molecules and the 3D structure of human FXa (PDB code: 1FJS),[35] suggested that *meta*-R-substituted (e.g., R = phenyl, **7d**) benzyloxy anilides of isonipecotic acid have potential for binding into the FXa catalytic cavity. Figure 1 shows the QXP-calculated docking pose of the representative isonipecotanilide inhibitor *N*-{[3-(1,1′-biphenyl-4-yl)methoxy]phenyl}piperidine-4-carboxamide (**7d**) into the binding pocket of human FXa, highlighting the importance of interactions (salt bridge, H-bonds) between the protonated piperidine (P_1) and Asp189 in S_1, whereas the P_4 phenyl group is embedded into the S_3/S_4 site, which is a box-shaped aromatic/hydrophobic cavity lined by residues Trp215, Tyr99, and Phe174.

We systematically explored the effects on the antiplatelet activity and FXa/thrombin inhibition of attaching the basic amidine group at P_1, and taking into account the effect of aromatic fluorine/s in increasing the potency of FXa[36] and thrombin[37] inhibitors, we introduced various fluorinated 1,1′-biphenyl as P_3/P_4 moiety. Herein, we report synthesis, in vitro biological activity, structure−activity relationships (SARs), and molecular modeling, highlighting our progress toward the above goal.

Chemistry

The nipecotamide- (**5**, **6**) and isonipecotamide-based derivatives (**7**, **8**) investigated in this study were synthesized as shown in Schemes 1 and 2. According to Scheme 1, the preparation of 1-(benzyloxy)-3-nitrobenzene (**3a**), its para isomer, and related congeners (**3b**−**e**, structural details in Table 1) was achieved upon reaction of 3(or 4)-nitrophenol with suitable benzyl bromide in dry DMF in the presence of K_2CO_3 (**3a**−**c**), or alternatively (**3b**−**e**) through a Mitsunobu reaction between 3(or 4)-nitrophenol and 1,1′-biphenyl-4-ylmethanol, using triphenylphosphine and diisopropyl azodicarboxylate (DIAD).[38] Reduction of the nitro group in **3a**−**e** with hydrazine hydrate and Raney nickel in refluxing MeOH[39] afforded the corresponding anilines **4a**−**e**, which were coupled in the subsequent step with the *N*-Boc-protected nipecotic and isonipecotic acids,[33] previously activated via acyl chloride (fluorinated derivatives **b** and **c**) or mixed anhydride formation (**a**, **d**, and **e**) using benzyl chloroformate, with satisfactory yields (45−85%). The Boc group was then removed with HCl gas in $CHCl_3$ solutions of the Boc-protected intermediates, affording the target anilide derivatives **5a**−**e** and **7a**−**e** as hydrochloride salts. Reaction of compounds **5b**,**d** and **7b**,**d** with *N*,*N*′-bis-Boc-*S*-methylthiopseudourea and $HgCl_2$ in dry DMF, and subsequent Boc removal with HCl gas, yielded the corresponding guanidine derivatives **6** and **8**, respectively.

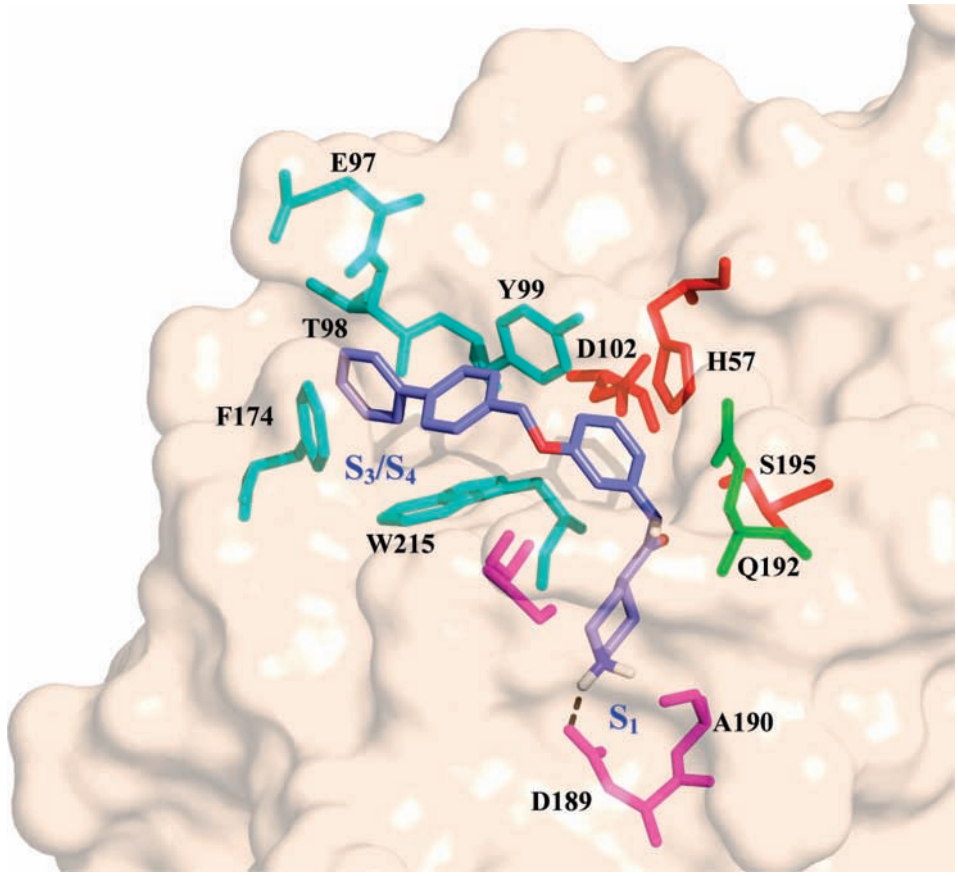

Figure 1. QXP highest scored docking pose of the designed isonipecotanilide inhibitor **7d** in stick (blue: nitrogen; red: oxygen; light blue: carbon atoms) into the binding pocket of human FXa (PDB: 1FJS). The protein surface is shown together with the main residues of the subsites S_1 (magenta) and S_3/S_4 (cyan). The catalytic triad (red-colored residues) and Q192 (green) are also shown. The figure was drawn by PyMOL.[36]

Unfortunately, following the pathway illustrated in Scheme 1, the isonipecotamide derivatives bearing fluorinated 1,1′-biphenyl as P_4 moieties (**7f**−**p**) were obtained in poor yields. They were then synthesized with moderate-to-good yields through an alternative pathway (Scheme 2), where the Boc-protected *N*-[3-(benzyloxy)phenyl]piperidine-4-carboxamide **7a** was first debenzylated by hydrogenolysis and the hydroxyphenyl intermediate **9** was alkylated with the suitable fluorinated 4-(bromomethyl)-1,1′-biphenyl. All the F-substituted 4′-bromomethylbiphenyl derivatives used for preparing compounds **7f**−**p** were already known,[40] and were synthesized in this study according to a reported Pd-catalyzed Suzuki cross-coupling reaction,[41] followed by bromination of the 4′-Me group with *N*-bromosuccinimmide (NBS).

Results and Discussion

The newly synthesized compounds were assayed for their antiplatelet activity on the in vitro aggregation of human platelet-rich plasma (PRP) induced by 10 μM ADP, using the Born's turbidimetric method.[42] Ten compounds were also tested for their activities against 10 μM EPN-induced PRP aggregation. The aggregation tracing relative to the controls with both agonists revealed a typical biphasic aggregation wave, which is more pronounced with EPN. At higher concentrations of nipecotamides (**5**) and isonipecotamides (**7**), both phases were inhibited. The platelet aggregation inhibition data, expressed as the IC_{50} (μM) values, represent the means ± SEM of at least three individual determinations, each performed in duplicate. Only compound **6d**, showing much less than 50% inhibitory effects at 1 mM concentration, was not examined for dose−response relation. The nipecotanilide derivative **2b** has been reassayed in this study as reference standard, and in Table 1, two other previously reported compounds (**2a** and **2c**)[33] have been included for comparison.

As a matter of fact, all the compounds tested against both agonists attained 50% inhibition activity of the EPN-induced PRP aggregation at concentrations 1.3−2.5 times lower than those required for inhibiting the ADP-induced aggregation; the EPN and ADP pIC_{50} values resulted linearly correlated with a close-to-one slope value and high correlation coefficient (r^2 = 0.954). It is known that the first low deflection of the aggregation wave in the EPN-induced platelet aggregation accounts for the formation of small aggregates, whereas their fusion into larger ones contributes to the second phase, which largely depends upon TxA_2 production and ADP release. Taking into account previous findings and the results of this study, such high correlation between EPN and ADP IC_{50} values suggests that most likely they exert inhibitory effects on EPN-induced aggregation, mainly interfering with the ADP-related signal transduction pathway. The overall amount of ADP released during EPN-induced aggregation is expected to be quite smaller than that used in our ADP assay, and this may explain the magnitude of EPN IC_{50} values, which were found lower than the values correspondingly determined in the ADP-induced aggregation test.

The lipophilicity of the investigated compounds was assessed by a reversed-phase (RP)-HPLC method,[33b,43] and the log values of polycratic capacity factors (log k'_w), that is capacity factors extrapolated at 100% aqueous mobile phase (pH 5.0), reported in Table 1.

Scheme 1[a]

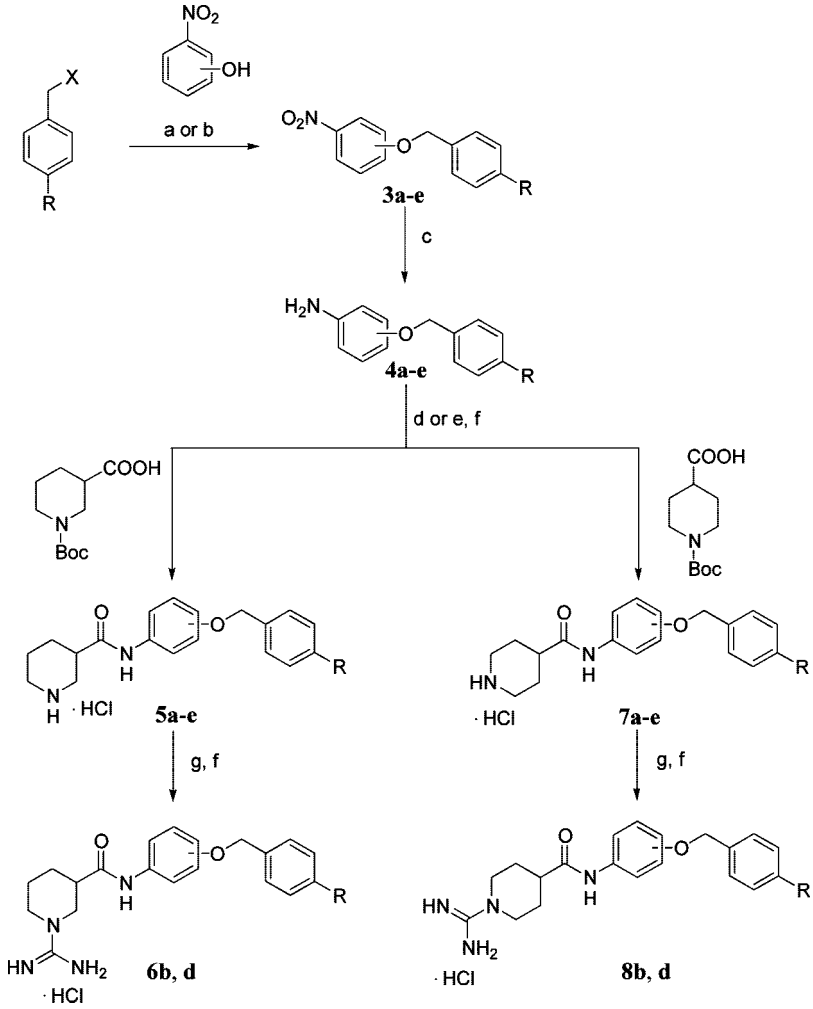

[a] Reagents and conditions: (a) X = Br, K_2CO_3, dry DMF, room temperature, 12 h, 85%; (b) X = OH, PPh_3, DIAD, dry THF, room temperature, 48 h, 62−66%; (c) $H_4N_2 \cdot H_2O$, Raney-Ni, MeOH, reflux, 2−4 h, 58−98%; (d) R = H or C_6H_5, BnOCOCl, TEA, dry THF, room temperature, 12 h; (e) R = F, $SOCl_2$, dry THF, TEA, room temperature, 12 h; (f) $CHCl_3$, HCl gas, 0 °C, 45−85%; (g) *N*,*N*′-bis-Boc-*S*-methylthiopseudourea, $HgCl_2$, dry DMF, 0 °C to room temperature, 24 h, 63−75%.

Scheme 2[a]

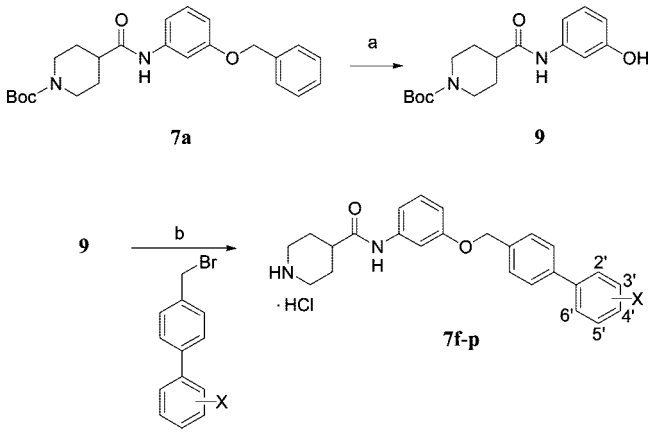

[a] Reagents and conditions: (a) H_2, 10% Pd/C, EtOH, room temperature, 12 h, 98%. (b) (i) NaH, dry DMF, room temperature, overnight; (ii) $CHCl_3$, HCl gas, 0 °C, 48−62%.

From the SAR viewpoint, data in Table 1 show that, albeit less lipophilic, benzyloxy anilides are almost equipotent with the *n*-hexyloxy congeners. With one exception (**7a**), the isonipecotoyl derivatives are equipotent or slightly more potent than the isomeric nipecotoyl congeners, the *meta*-substituted derivatives (**7b** and **7d**) displaying better antiplatelet properties than the para positional isomers (**7c** and **7e**).

Interestingly, a fluorine substituent at the para position of the benzyl group favorably affected the potency of the examined piperidine carboxamides, such an effect being particularly strong with 3-(4-fluorobenzyl)oxy isonipecotanilide **7b**, which resulted the most promising antiplatelet agent in Table 1 (IC_{50} values of 68 and 36 μM against ADP- and EPN-induced PRP aggregations, respectively). In contrast, a sharp decrease of antiplatelet potency was observed for the amidine-bearing (N1−C(NH)NH_2) derivatives **6** and **8**; their potency was 3−10 times lower than that of the corresponding more lipophilic N1−H derivatives **5** and **7**.

In agreement with previous findings,[32,33b] most of the N1−H nipecotamides (**2** and **5**) and isonipecotamides (**7**) lie on a parabolic curve correlating pIC_{50} with the lipophilicity parameter log k'_w, and indeed the following parabolic equation, explaining more than 80% of the variance in the activity data, was obtained by regression analysis of the N1−H data set:

$$pIC_{50} = 1.03\ (\pm 0.16)\ \log k'_w - 0.15\ (\pm 0.03)(\log k'_w)^2 + 2.29\ (\pm 0.22)$$
$$n = 13\ r^2 = 0.8435\ s = 0.1226\ F = 26.95 \quad (1)$$

Table 1. Platelet Aggregation Inhibitory Activities, Inhibition Constants for Factor Xa (FXa) and Thrombin (FIIa) and Lipophilicity Parameters of Benzyloxyphenyl Piperidine Carboxamides[a]

				IC_{50},[c] μM		K_i,[d] μM	
compd	3 or 4 position	R	log k'_w[b]	ADP	EPN	FXa	FIIa
2a[e]	4		0.79	983 ± 20***	n.d.[g]	n.d.	n.d.
2b[e]	4		3.53	85 ± 12	43 ± 9	*f*	*f*
2c[e]	3		3.75	113 ± 17	n.d.	*f*	*f*
5a	3	H	2.44	128 ± 19	n.d.	*f*	*f*
5b	3	F	2.67	103 ± 16	70 ± 8	260	*f*
5c	4	F	2.41	116 ± 6	90 ± 11*	*f*	*f*
5d	3	C_6H_5	4.50	153 ± 12*	87 ± 13	2.50	*f*
5e	4	C_6H_5	4.30	125 ± 15	n.d.	*f*	*f*
6b	3	F	2.82	274 ± 26*	n.d.	57.0	160
6d	3	C_6H_5	4.57	>1000	n.d.	2.00	31.3
7a	3	H	2.47	229 ± 30**	n.d.	*f*	*f*
7b	3	F	2.61	68 ± 13	36 ± 3	*f*	*f*
7c	4	F	2.35	121 ± 11	93 ± 10*	*f*	*f*
7d	3	C_6H_5	4.45	111 ± 8*	54 ± 6	1.00	*f*
7e	4	C_6H_5	4.18	135 ± 20	n.d.	126	*f*
8b	3	F	2.76	768 ± 40***	n.d.	33.8	20.8
8d	3	C_6H_5	4.67	400 ± 20**	244 ± 8**	5.20	40.4

[a] General structures in Scheme 1. [b] Log of RP-HPLC polycratic capacity factor, i.e., capacity factor extrapolated at 100% aqueous mobile phase (variable fraction of MeOH in 40 mM ammonium acetate solution, pH = 5.0); stationary phase: Phenomenex Gemini C18 column (150 mm × 4.6 mm i.d., 5 μm particles). [c] Compound concentration which inhibits ADP- and EPN-induced platelet aggregation by 50% in a PRP assay. Data are means ± SEM of at least three different determinations, each performed in duplicate; *$p < 0.05$, **$p < 0.01$, ***$p < 0.001$ significantly different from compound **2b**. [d] In vitro inhibition constants from amydolitic assay. [e] Previously reported[33] *N*-(4-methoxyphenyl)- (**2a**), *N*-(4-hexyloxyphenyl)- (**2b**), and *N*-(3-hexyloxyphenyl)piperidine-3-carboxamides (**2c**); compd **2b** has been tested in this study as a reference standard. [f] Less than 30% inhibition at the maximum concentration tested (250 μM). [g] n.d. = not determined.

where *n* represents the number of data points, r^2 the squared correlation coefficient, *s* the standard deviation of the regression equation, *F* the statistical significance of fit; 95% confidence intervals of the regression coefficients are given in parentheses.

The above relationship between antiplatelet potency data and lipophilicity parameters of piperidine-3 (or 4-)-carboxamides is consistent with the postulated mechanism of action[32,33] in which (i) penetration through the lipid bilayer of the platelet membrane should be a critical step and (ii) interaction with anionic PLs (in particular with phosphoinositides, which are major components of the platelet membrane) triggers a number of processes leading to the inhibition of platelet activation and aggregation. In both steps, kinetics of adsorption to and translocation through platelet membranes, as well as micelle formation and/or limited solubility of more lipophilic analogues, could be responsible for the parabolic lipophilicity−activity relationship.

The four guanidine derivatives **6b**,**d** and **8b**,**d** do not fit the parabolic eq 1. An argument that can shed light on the different behavior shown by amine or guanidine derivatives is offered by a recent study of Kooijman et al.,[44] who investigated specific interactions between lysine (primary amine) and arginine (guanidine) side chains with the phosphate headgroup of phosphatidic acid (PA), a minor but important PL playing a central role in several key cellular processes through specific interactions with proteins. Lys and Arg residues increase the charge of PA from −1 to −2, predominantly by forming hydrogen bonds (HBs), thereby stabilizing the protein−lipid interactions. Lys residues, which are likely stronger HB donors than Arg residues, as on the other hand supported by search of Cambridge Structural database and molecular dynamics simulations, proved to be more effective in docking the phosphomonoester headgroup of PA. Phosphomonoesters occur not only in PA, but also in other anionic PLs, such as phosphatidyl inositol mono-, bi-, and triphosphate, bearing $-OPO_3H^-$ moiety(ies) at the position 3, 4, and/or 5 of the inositol fragment. Binding of our N1−H and N1−C(NH)NH_2 (iso)nipecotamide derivatives, both protonated at physiological pH, to the phosphomonoester moiety(ies) of the anionic PLs should be reasonably regulated by similar principles. A stronger interaction of the secondary amino group in the (iso)nipecotamide derivatives **2**, **5**, and **7** with the phosphate headgroup in the anionic PLs of the platelet membrane could likely explain their higher activity compared with that of the guanidine derivatives **6** and **8**.

The compounds in Table 1 were then evaluated in vitro for inhibition of FXa and thrombin and their potencies expressed as inhibition constants (K_i, μM). Only four compounds, namely **5d**, **6d**, **7d**, and **8d**, all bearing 1,1′-biphenyl as P_3-P_4 moiety, showed FXa inhibition constants in the low micromolar range (K_i values ranging from 1.00 to 5.20 μM). Interestingly, the *meta*-substituted derivatives (**5d** and **7d**) proved to be hundred-fold more potent than the *para*-substituted ones (**5e** and **7e**). Although guanidine derivatives **6d** and **8d** were almost equipotent with **5d** and **7d** against FXa, the selectivity versus thrombin was only 15-fold and 8-fold, respectively. The achiral isonipecotoyl derivative **7d** is noteworthy for FXa inhibition potency and selectivity and was chosen as lead for further optimization.

In an attempt to improve binding of the P_4 moiety of **7d** into the "aryl binding site" of FXa, we replaced hydrogen/s of the distal phenyl with fluorine/s. Actually, fluorine substitution has become increasingly a successful strategy for lead optimization in several cases.[45] The substitution of hydrogen with fluorine generally results in minimal steric effects, while a number of properties contributing to the ability of a molecule to engage in intermolecular interactions, such as dipole moment, electrostatic distribution, aromatic−aromatic interactions, hydrogen bonding, and lipophilicity, can be significantly modulated.[46] Evidence has been reported in literature proving implication of aromatic F in the enzyme−ligand binding affinity and selectivity of thrombin[38,47] and factor Xa inhibitors.[37]

Eleven fluorinated 3-(biphenyl-4-ylmethoxy)phenyl piperidine-4-carboxamides (**7f**−**p**), including monofluoro (**7f**−**h**), difluoro (**7j**−**m**), trifluoro (**7n**−**o**), and one 4-trifluoromethyl (**7p**) congeners, were tested in vitro for inhibition of FXa, thrombin (FIIa), and α-chymotrypsin (α-CT), and some of them, including the most potent FXa inhibitors, for inhibition of platelet aggregation (Table 2).

Table 2. Platelet Aggregation Inhibitory Activities, Inhibition Constants for FXa, FIIa, and α-Chymotrypsin (α-CT), and Lipophilicity Parameters of Fluorinated 3-(Biphenyl-4-ylmethoxy)phenyl Piperidine-4-carboxamides[a]

			IC_{50}, μM[c]		K_i, μM[d]		
compd	X	log k'_w[b]	ADP	EPN	FXa	FIIa	α-CT
7f	4′-F	4.74	35 ± 15**	19 ± 5*	3.87	*e*	*e*
7g	3′-F	5.07	34.7 ± 5**	14.4 ± 3***	0.177	*e*	31.0
7h	2′-F	4.87	62.7 ± 9	n.d.[f]	0.767	*e*	*e*
7j	2′,4′-F_2	5.06	98.8 ± 14	n.d.	0.512	54.0	*e*
7k	2′,3′-F_2	5.05	n.d.	n.d.	0.548	*e*	60.0
7i	2′,5′-F_2	4.98	n.d.	n.d.	1.27	*e*	*e*
7l	2′,6′-F_2	4.72	n.d.	n.d.	1.45	*e*	*e*
7m	3′,5′-F_2	4.93	27.8 ± 4***	17 ± 3***	0.130	*e*	60.3
7n	2′,4′,6′-F_3	4.61	n.d.	n.d.	9.47	26.7	*e*
7o	3′,4′,5′-F_3	5.21	76.7 ± 15	n.d.	0.666	*e*	*e*
7p	4′-CF_3	5.93	65.7 ± 13	n.d.	0.057	*e*	*e*

[a] General structure in Scheme 2. [b] Log of RP-HPLC polycratic capacity factor, i.e., capacity factor extrapolated at 100% aqueous mobile phase (variable fraction of MeOH in 40 mM ammonium acetate solution, pH = 5.0); stationary phase: Phenomenex Gemini C18 column (150 mm × 4.6 mm i.d., 5 μm particles). [c] Compound concentration which inhibits ADP- and EPN-induced platelet aggregation by 50% in a PRP assay. Data are means ± SEM of at least three different determinations, each performed in duplicate; *p < 0.05, **p < 0.01, ***p < 0.001 significantly different from compound **2b**. [d] In vitro inhibition constants from amydolitic assay. [e] Less than 30% inhibition at the maximum concentration tested (250 μM). [f] n.d. = Not determined.

Among the monofluorinated derivatives, when compared with the unsubstituted parent compound **7d**, only the 3′-F congener (**7g**) resulted in 6-fold ($\Delta\Delta G \approx 1$ kcal·mol^{-1}) greater potency although showing limited selectivity against α-CT, whereas the 2′-F isomer (**7h**) did not show any appreciable increase of FXa inhibitory potency and the 4′-F one (**7f**) proved to be about 4-fold less potent. Our results showed that di- and trifluorinated derivatives, with the exception of the 3′,5′-difluorinated congener with about 8-fold increase of potency (**7m**), have a potency similar to or lower than that of nonfluorinated **7d**. Double fluorination at the ortho positions (**7l**), and even more addition of three fluorines in the ortho and para positions (**7n**), proved to be deleterious, the last showing a drop of FXa potency and selectivity against thrombin. As opposed to the *para*-monofluorinated derivative **7f**, the 4′-CF_3 congener **7p** was much more potent ($\Delta\Delta G \approx 2$ kcal·mol^{-1}) than the parent analogue **7d**. Compound **7p**, with a K_i value of 57 nM, is to date our most potent FXa inhibitor, displaying more than 4400-fold selectivity against both FIIa and α-CT.

The binding mode into the binding site of FXa of the most active inhibitors **7g**, **7m**, and **7p**, compared with that of the parent compound **7d**, was investigated by docking calculations. The X-ray structure of human FXa (PDB code 1FJS; 1.92 Å resolution),[35] in complex with the inhibitor ZK-807834 (CI-1031), was retrieved from the Brookhaven Protein Data Bank and used in the calculations with QXP software.[34] The docking poses corresponding to the highest scored solutions of **7m** (very similar to those of **7d** and **7g**) and **7p** are shown in Figure 2. In the lowest-energy enzyme−ligand complexes, the conformations of all the investigated compounds docked to the FXa are similar with respect to the bend between the protonated piperidine (P_1) and the fluorinated 1,1′-biphenyl (P_3−P_4) moieties.

All the binding models show two main common interactions: (i) salt bridge, strengthen by HBs, between the piperidinium group, in "chair" conformation, and the carboxylate of Asp189 at the bottom of the enzyme S_1 pocket (average distance 3.3 Å), and (ii) HB between the amide carbonyl of the ligand and the catalytic residue Ser195 of FXa (O···O average distance and O−H···O angle about 2.8 Å and 160°, respectively). The models show a possible aromatic ring-stacking between the distal phenyl group (P_4) and the S_4 pocket, that is a narrow hydrophobic channel lined by aromatic side chains of Tyr99, Phe174, and Trp215. In particular, for **7d**, **7g**, and **7m**, which adopt closely superimposed conformations, the distal phenyl ring, deeply inside the S_4 aryl binding site, is sandwiched between the aromatic rings of Tyr99 and Phe174, likely through $\pi-\pi$ interactions, and makes CH−π interactions with the indole ring of Trp215. In contrast, the distal 4′-CF_3-phenyl of **7p** is shifted ahead and rotated, achieving face-to-face aromatic interaction with Trp215.

We believe that the positioning of the F atoms in **7g**, **7m**, and **7p**, with their propensity to engage polar interactions with the backbone CO (and NH) groups inside the S_4 pocket (i.e., the so-called "fluorophilic" interactions), may be a determinant for the increase of their inhibition potency. In particular, for the most potent inhibitor **7p**, the computational model identifies two middle-range contacts between C(sp^3)-F and CO moieties of Thr98 (d: 2.9 Å, θ: 40°) and Glu97 (d: 3.8 Å, θ: 25°), whose geometries (e.g., θ values less than the magic angle, which is approximately 54.7°) would be suitable for allowing attractive C(sp^3)-F···C═O dipole−dipole interactions.

The prolongation of the activated partial tromboplastin time (aPTT) in human plasma was also measured for the most potent inhibitors **7g**, **7m**, and **7p** in order to determine their in vitro anticoagulant activity (defined as the inhibitor concentration required to increase aPTT by 2-fold). The aPTT identifies the time interval required for clot formation in response to a nonphysiological stimulus, such as kaolin, which leads to primary activation of the intrinsic or contact pathway. In our assay conditions, the aPTT was doubled at concentrations only in the high micromolar range (140 μM for **7p**, 190 μM for **7m**, and 205 μM for **7g**; **7a** did not show any effect on the aPTT up to 1 mM concentration).

Finally, a number of fluorinated isonipecotamide derivatives **7** in Table 2 were assayed for the ability to inhibit in vitro the ADP (and EPN in a fewer cases)-induced human platelet aggregation. All the tested compounds inhibited platelet aggregation with potency higher than that of the unsubstituted analogue **7d**, their IC_{50} values ranging from 28 to ca. 100 μM. Such an increase in antiplatelet potency was not expected based only on the small increase of lipophilicity and the parabolic eq 1. We recalculated the second-order curve regression with log k'_w for the whole series of the N1−H piperidine-(3 and 4)-carboxamides (i.e., combining the antiaggregatory activity data of compounds **2**, **5**, and **7** from Table 1 and fluorinated congeners **7** from Table 2) and incorporated into the regression model favorable and detrimental effects, using the following indicator (or category) variables: I_F accounting for fluorination (it assumes the value 1 for fluorinated and 0 for nonfluorinated compounds), and I_o accounting for detrimental F-substitution

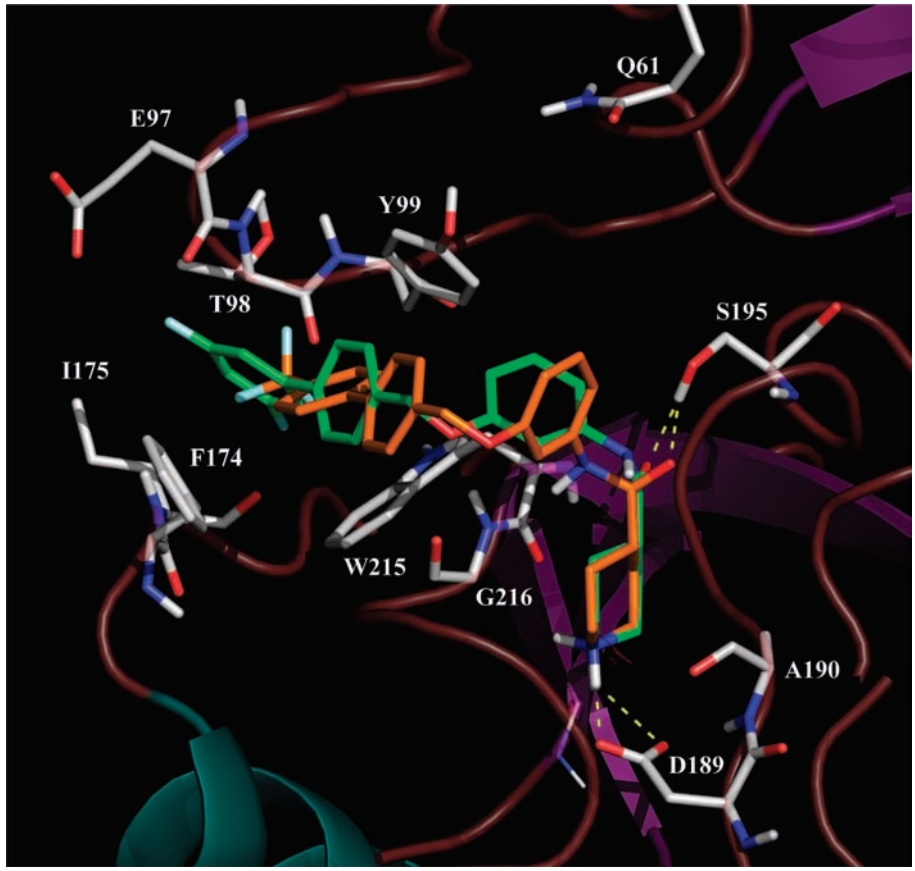

Figure 2. Overlay of compounds **7m** and **7p** docked into the binding site of factor Xa (PDB code: 1FJS). The QXP highest scored docking poses are shown. The figure was drawn by PyMOL.[36] The protein is shown in ribbon, and the ligands and potentially interacting residues in stick (blue: nitrogen; red: oxygen; green: carbon atoms in **7m**; orange: carbon atoms in **7p**).

in the ortho positions (−1 for *ortho*-substituted congeners, 0 for the others). A stepwise multiple regression analysis yielded the following equation:

$$\mathrm{pIC_{50}} = 0.64\ (\pm 0.13)\ \log k'_w - 0.07\ (\pm 0.02)(\log k'_w)^2 + 0.34\ (\pm 0.06)(I_F - I_o) + 2.54\ (\pm 0.21)$$
$$n = 20\ r^2 = 0.8458\ s = 0.1406\ F = 29.26 \quad (2)$$

The substitution of H with F can improve the interaction of these derivatives (predominantly in the piperidinium form at the physiological pH) with platelet membranes, more than expected from the lipophilicity parameter alone. Indeed, studies of transport kinetics of lipophilic ions across plasma membranes proved the translocation of the F-substituted congeners to be slower than that of the parent hydrogenated ones by at least 1 order of magnitude.[48] Such a kind of "extralipophilic" effect due to the F-substitution should add significantly to the antiplatelet activity of the 4-carboxypiperidinium derivatives **7**.

Taking all the above findings into account, three isonipecotamide-containing compounds, namely the *meta*-fluorinated derivatives **7g** (K_i (FXa) = 0.177 μM, IC_{50} (ADP) = 34.7 μM) and **7m** (K_i (FXa) = 0.130 μM, IC_{50} (ADP) = 27.8 μM), and the *para*-trifluoromethyl congener **7p** (K_i (FXa) = 0.057 μM, IC_{50} (ADP) = 65.7 μM) as well, which proved to be good FXa and moderate platelet aggregation inhibitors, can be chosen as leads for further optimization of novel dual-function antithrombotic agents. Among them, the 4′-CF_3 congener **7p**, displaying >4400-fold selectivity for FXa versus thrombin and chymotrypsin, is noteworthy.

Conclusions

Introducing suitable modifications into the structure of lipophilic nipecotic acid anilides,[33] previously identified as in vitro inhibitors of blood platelet aggregation, we succeeded in the purpose of empowering these molecules with anticoagulant activity, achieved by the selective inhibition of factor Xa of the blood coagulation cascade. The combination of FXa inhibition and platelet antiaggregatory activities into one molecule, which per se should be advantageous (as for pharmacokinetics, drug interactions and toxicity, less demanding clinical studies, etc.), can enhance its potential as antithrombotic agent in patients with prosthetic heart valves and atrial fibrillation.

Our study led to the development of some fluorinated benzyloxyphenyl piperidine-4-carboxamides (**7**), able of acting in vitro both as FXa inhibitors, with potency in the nanomolar range, and inhibitors of ADP-induced platelet aggregation, with potency in the micromolar range.

A major outcome of this study was the identification of two fluorinated derivatives of *N*-[3-(biphenyl-4-yl)-phenyl]piperidine-4-carboxamide, **7m** (3′,5′-F_2 congener) and **7p** (4′-CF_3 congener), which proved to be potent and selective inhibitors of FXa, additionally endowed with a moderate-to-good antiplatelet activity. These new dual-function agents, albeit still requiring optimization of potency and selectivity, can be

considered promising leads in the search for new efficacious and safe antithrombotic drugs.

Experimental Section

Chemistry. Melting points were determined by using the capillary method on a Stuart Scientific SMP3 electrothermal apparatus and are uncorrected. Elemental analyses (C, H, N) were performed on an Euro EA3000 analyzer (Eurovector, Milan, Italy) using the Analytical Laboratory Service of the Dipartimento Farmaco-chimico of the University of Bari, and the results agreed to within ±0.40% of the theoretical values. Mass spectra were recorded on Agilent GC-MS 689-973. IR spectra were recorded using KBr disks on a Perkin−Elmer Spectrum One FT-IR spectrophotometer (Perkin−Elmer Ltd., Buckinghamshire, UK), and the most significant absorption bands are listed. ^{1}H NMR spectra were recorded at 300 MHz on a Varian Mercury 300 instrument. Chemical shifts are expressed in δ and the coupling constants J in hertz. The following abbreviations are used: s, singlet; d, doublet; t, triplet; m, multiplet. Signal due to NH and OH protons were located by deuterium exchange with D_2O.

Chromatographic separations were performed on silica gel 60 for column chromatography (Merck 70−230 mesh, or alternatively 15−40 mesh for flash chromatography). Unless otherwise stated, starting materials, and all chemicals and solvents as well, were purchased from Sigma-Aldrich. Several compounds were synthesized according to known procedures with slight modifications; their melting points and spectral data were in full agreement with those reported in literature, and no effort was made at this stage to optimize the yields.

General Procedure for Synthesis of 3- or 4-[(4-*R*-benzyl)-oxy]anilines (4). The synthesis of 3-benzyloxyaniline (**4a**) is reported as an example. Dry potassium carbonate (1.2 g, 8.63 mmol) was added to a solution of 3-nitrophenol (1.0 g, 7.19 mmol) in 7 mL of dry DMF. After 30 min, a solution of benzyl bromide (0.94 mL, 7.91 mmol) in 3 mL of dry DMF was added dropwise, and the suspension was stirred at room temperature overnight. The reaction was quenched by addition of 100 mL of water, and the resulting mixture was extracted with ethyl acetate (3 × 20 mL). The combined organic extracts were then washed with brine, dried (Na_2SO_4), and concentrated under reduced pressure. The resultant yellow solid was crystallized from ethanol to afford 1.4 g (85% yield) of 1-(benzyloxy)-3-nitrobenzene (**3a**).

A mixture of **3a** (1.4 g, 6.10 mmol), hydrazine hydrate (1.5 mL, 30.3 mmol), and activated Raney nickel suspension (1 mL) in 100 mL of methanol was heated at reflux for 2 h, until starting material disappeared on TLC. The cooled mixture was filtered through a pad of celite and the filtrate concentrated under reduced pressure to afford the target compound **4a** in almost quantitative yield.

Physical data, IR and ^{1}H NMR spectra of 1-(benzyloxy)-3-nitrobenzene (**3a**), 1-[(4-fluorobenzyl)oxy]-3-nitrobenzene (**3b**), 1-[(4-fluorobenzyl)oxy]-4-nitrobenzene (**3c**), and corresponding amino derivatives (**4a**−**c**) were in good agreement with the reported ones.[40,49−51]

(1,1′-Biphenyl-4-yl)methyl 3-nitrophenyl ether (3d). Diisopropyl azodicarboxylate (DIAD, 1.42 mL, 7.19 mmol) was added dropwise at 0 °C to a stirred solution of 3-nitrophenol (1.0 g, 7.19 mmol), triphenylphosphine (1.9 g, 7.19 mmol), and (1,1′-biphenyl-4-yl)methanol (1.3 g, 7.19 mmol) in 20 mL of dry THF, and the mixture was stirred for about 48 h at room temperature. The solvent was removed by evaporation under reduced pressure, and the oil residue was purified by chromatography on silica gel, eluting with petroleum ether/ethyl acetate (90:10, v/v), to afford 1.44 g (66% yield) of the crude product as a pale-yellow solid; mp 126−129 °C, from petroleum ether/AcOEt. ^{1}H NMR ($CDCl_3$) δ 7.96 (d, 1H, J = 8.0 Hz), 7.5−7.68 (m, 8H), 7.45 (t, 1H, J = 7.7 Hz), 7.37 (d, 1H, J = 7.1 Hz), 7.15 (d, 1H, J = 8.2 Hz), 7.05 (t, 1H, J = 8.0 Hz), 5.28 (s, 2H). IR (cm^{-1}) 1532, 1518, 1353, 1247, 1028, 861, 814, 763.

(1,1′-Biphenyl-4-yl)methyl 4-nitrophenyl ether (3e). Compound **3e** was synthesized from 4-nitrophenol according to the procedure described for **3d**.

3-[(1,1′-Biphenyl-4-yl)methoxy]aniline (4d). A mixture of **3d** (1.0 g, 3.28 mmol), hydrazine hydrate (1.1 mL, 22.9 mmol), and activated Raney nickel suspension (1 mL) in 100 mL of methanol was heated at reflux for 4 h until starting material disappeared on TLC. The cooled mixture was filtered through a celite pad and the filtrate concentrated under reduced pressure to afford an oil residue, which was purified by chromatography on silica gel, eluting with petroleum ether/ethyl acetate (90:10, v/v), to afford the crude title compound as a pale-brown solid (0.56 g, 62% yield). The raw material of **4d** was used in the next coupling reaction without further purification; mp 115−118 °C, from petroleum ether/AcOEt. ^{1}H NMR ($CDCl_3$) δ 7.67−7.59 (m, 5H), 7.52−7.42 (m, 4H), 7.35 (d, 1H, J = 6.9 Hz), 6.89 (d, 1H, J = 6.6 Hz), 6.69−6.85 (m, 2H), 5.13 (s, 2H), 4.00 (s, 2H). IR (cm^{-1}) 3462, 3368, 1624, 1596, 1190, 1010, 831, 752.

4-[(1,1′-Biphenyl-4-yl)methoxy]aniline (4e). Compound **4e** was synthesized by reduction of **3e** according to the procedure described for **4d**.

General Procedures for Synthesis of R-Substituted Benzyloxyphenyl Piperidine-4 (or 3-)-Carboxamides. Method A (5b−c, 7b−c, 7f). The synthesis of *N*-{3-[(4-fluorobenzyl)oxy]-phenyl}piperidine-3-carboxamide hydrochloride (**5b**) is reported as an example.

Thionyl chloride (1.4 mL, 19.3 mmol) was added to a cooled solution of *N*-Boc-nipecotic acid (1.1 g, 4.83 mmol) in 20 mL of dry THF. The reaction mixture was stirred at room temperature for 3 h, and the solvent was removed by evaporation under reduced pressure to give the acyl chloride product as a pale-yellow oil, which was dried in nitrogen atmosphere. The crude oil dissolved in 10 mL of dry THF was added dropwise to a solution of 4-(benzyloxy)aniline (0.70 g, 3.22 mmol) and triethylamine (1.35 mL, 9.66 mmol) in 15 mL of dry THF, and reaction mixture was stirred overnight at room temperature. The solid precipitate was filtered off and the filtrate concentrated under reduced pressure. The oil residue was dissolved in 50 mL of ethyl acetate and washed with 1 N HCl (3 × 20 mL), 5% (w/v) $NaHCO_3$ (3 × 20 mL) and finally with brine (3 × 20 mL). The organic phase was dried (Na_2SO_4) and evaporated in vacuo, yielding an oil residue, which was purified by silica gel column chromatography, eluting with petroleum ether/ethyl acetate (65:35, v/v) to afford the target *N*-Boc-protected anilide as a solid product. A solution of 1.0 mmol of the *N*-Boc-protected anilide in 30 mL of chloroform was cooled to 0−5 °C, saturated with HCl gas. Then the solvent was evaporated under reduced pressure, and the crude solid was purified by crystallization from ethanol/ethyl acetate to afford the hydrochloride salt of *N*-{3-[(4-fluorobenzyl)oxy]phenyl}piperidine-3-carboxamide (**5b**) as a white microcrystalline solid (85% yield); mp 219−220 °C. ^{1}H NMR (DMSO-d_6) δ 10.27 (s, 1H), 8.60 (s, 2H), 7.46 (t, 1H, J = 6 Hz), 7.38 (s,1H), 7.10−7.23 (m, 5H), 6.69 (d, 1H, J = 8 Hz), 5.02 (s, 2H), 3.29−3.32 (m, 2H), 3.13−3.17 (m, 2H), 2.46−2.49 (m, 1H), 1.48−1.77 (m, 4H). IR (cm^{-1}) 3541, 3322, 1663, 1225, 1154, 1039, 857, 825, 770. Anal. ($C_{19}H_{22}N_2O_2FCl$) C, H, N.

Method B (5a, 5d−e, 7a, 7d−e). . The synthesis of *N*-{[3-(1,1′-biphenyl-4-yl)methoxy]phenyl}piperidine-4-carboxamide hydrochloride (**7d**) is reported as an example.

A solution of benzyl chloroformate (0.63 mL, 4.36 mmol) in 5 mL of dry THF was added dropwise to a cooled solution of *N*-Boc-nipecotic acid (1.0 g, 4.36 mmol) and triethylamine (1.22 mL, 8.72 mmol) in 15 mL of dry THF. After 30 min of stirring at room temperature, a solution of 3-[(1,1′-biphenyl-4-yl)methoxy]aniline (1.2 g, 4.36 mmol) in 10 mL of dry THF was added, and the reaction mixture was stirred at room temperature overnight. The solid precipitate was filtered off and the filtrate concentrated under reduced pressure. The oil residue was dissolved in 50 mL of ethyl acetate and washed with 1 N HCl (3 × 20 mL), 5% w/v $NaHCO_3$ (3 × 20 mL), and finally with brine (3 × 20 mL). The organic phase was dried (Na_2SO_4) and evaporated in vacuo, yielding an oil residue, which was purified by silica gel column chromatography (mobile phase: petroleum ether/ethyl acetate, 80:20, v/v) to afford the target *N*-Boc-protected anilide as a solid product. The *N*-Boc carboxamide was deprotected with HCl gas, following a procedure

similar to that described above for **5b**, and the resultant residue was purified by crystallization from ethanol/ethyl acetate to give *N*-{[3-(1,1′-biphenyl-4-yl)methoxy]phenyl}piperidine-4-carboxamide hydrochloride salt (**7d**) as pale-brown crystals in 60% yield; mp 189−192 °C. ^{1}H NMR (DMSO-d_6) δ 10.12 (s, 1H), 8.78 (s, 2H), 7.67−7.63 (m, 4H), 7.51−7.32 (m, 6H), 7.21−7.12 (m, 2H), 6.70 (d, 1H, J = 9 Hz), 5.09 (s, 2H), 3.32−3.27 (m, 1H), 2.88 (t, 2H, J = 9 Hz), 2.58−2.65 (m, 1H), 1.71−1.95 (m, 5H). IR (cm^{-1}) 3466, 1663, 1284, 1224, 1156, 791, 753. Anal. ($C_{23}H_{27}N_2O_2Cl\cdot H_2O$) C, H, N.

General Procedure for Guanylation of Compounds 5 (6b, 6d) and 7 (8b, 8d). The synthesis of 1-[amino(imino)methyl]-*N*-{3-[(4-fluorobenzyl)oxy]phenyl}piperidine-4-carboxamide hydrochloride (**8b**) is reported as an example.

N,*N*′-bis-Boc-*S*-methylthiopseudourea (0.62 g, 2.14 mmol), triethylamine (0.75 mL, 5.34 mmol), and mercury(II) chloride (0.58 g, 2.14 mmol) were added in a sealed tube containing a cooled solution of **7b** (650 mg, 1.78 mmol) in 6 mL of dry DMF, and the reaction mixture was stirred for 3 h at 0 °C and 24 h at room temperature. Ethyl acetate (15 mL) was then added to the reaction mixture, and stirring was continued for 15 min. The precipitate was filtered off and washed 3 times with 15 mL of ethyl acetate. The combined organic phases were washed with brine (3 × 20 mL), dried (Na_2SO_4), and concentrated under reduced pressure to afford a residue, which was purified by silica gel column chromatography, eluting with petroleum ether/ethyl acetate (90:10, v/v). The Boc group was removed (HCl gas) to afford 0.46 g (63% yield) of the product HCl salt **8b** as white microcrystalline solid; mp 239−241 °C, from EtOH. ^{1}H NMR (DMSO-d_6) δ 10.37 (s, 1H), 7.54 (s, 4H), 7.49−7.37 (m, 3H), 7.22−7.11 (m, 4H), 6.66 (d, 1H, J = 7 Hz), 5.02 (s, 2H), 3.88 (d, 2H, J = 14 Hz), 3.05 (d, 1H, J = 14 Hz), 3.01 (d, 1H, J = 14 Hz), 2.70−2.55 (m, 1H), 1.90−1.75 (m, 2H) 1.58- 1.45 (m, 2H). IR (cm^{-1}) 3333 1654, 1224 1154 1039, 825, 775. Anal. ($C_{20}H_{24}N_4O_2FCl\cdot H_2O$) C, H, N.

***tert*-Butyl 4-[*N*-(3-Hydroxyphenyl)carbamoyl]piperidine-1-carboxylate (9).** A suspension of *tert*-butyl 4-{[3-(benzyloxy)phenyl]-carbamoyl}piperidine-1-carboxylate **7a** (2.1 g, 5.24 mmol) and 0.10 g of 10% palladium on carbon charcoal in 50 mL of ethanol was stirred at room temperature in hydrogen atmosphere until starting material disappeared on TLC. The reaction mixture was filtered through a pad of celite, and the solvent was removed by evaporation under reduced pressure to give **9** as a brown solid in almost quantitative yield. Compound **9** was used in the subsequent reactions without further purification. ^{1}H NMR (DMSO-d_6) δ 9.75 (s, 1H), 9.30 (s, 1H), 7.15 (m, 1H), 7.02 (t, 1H, J = 9 Hz), 6.93 (d, 1H, J = 9 Hz), 6.40 (d, 1H, J = 9 Hz), 3.97 (d, 2H, J = 14 Hz), 2.80−2.73 (m, 2H), 2.55−2.45 (m, 1H), 1.80−1.65 (m, 2H), 1.52−1.48 (m, 2H), 1.38 (s, 9H). IR (cm^{-1}) 3240, 1663, 1278, 1222, 1160, 781.

Synthesis of Fluorinated 4′-(Bromomethyl)-1,1′-biphenyl Congeners. The preparation of 4′-(bromomethyl)-3-fluoro-1,1′-biphenyl is reported as representative example. *N*-bromosuccinimmide (1.5 g, 8.70 mmol) was added to a solution of 3-fluoro-4′-methyl-1,1′-biphenyl (1.6 g, 8.70 mmol), which in turn was prepared according to a reported method[52] in 30 mL of CCl_4. The reaction mixture was refluxed for 20 h and then allowed to cool to room temperature. The insoluble succinimmide was filtered off and the solvent was evaporated under reduced pressure to yield 2.1 g (90% yield) of the target compound as a crude oil, which was used without further purification. ^{1}H NMR ($CDCl_3$) δ 7.71 (d, 2H, J = 8 Hz), 7.53−7.48 (m, 4H), 7.21−7.11 (m, 2H). IR (cm^{-1}) 2950, 1485, 820, 765.

General Procedure for Synthesis of Compounds 7f−p. The synthesis of *N*-{3-[(3′-fluoro-1,1′-biphenyl-4-yl)methoxy]phenyl}-piperidine-4-carboxamide·HCl (**7g**) is reported as a representative example.

A solution of *tert*-butyl 4-[*N*-(3-hydroxyphenyl)carbamoyl]piperidine-1-carboxylate **9** (0.60 g, 1.89 mmol) in 5 mL of dry DMF was added to a suspension of NaH (0.68 g, 2.84 mmol) in 3 mL of dry DMF at room temperature. After 15 min, a solution of 4′-(bromomethyl)-3-fluoro-1,1′-biphenyl (0.50 g, 1.89 mmol) in 5 mL of dry DMF was slowly added dropwise, and the reaction mixture was stirred for 6−8 h at room temperature. The reaction was quenched by adding 5 mL of 5% (w/v) $KHSO_4$ and, after 5 min, diluted with 50 mL of distilled water. The aqueous phase was then extracted with ethyl acetate (3 × 15 mL), and the combined organic extracts were washed twice with brine, dried (Na_2SO_4), and concentrated under reduced pressure. The residue was purified by silica gel column chromatography, eluting with petroleum ether/ethyl acetate (90:10, v/v), and the chromatographically pure *N*-Boc protected derivative was treated with HCl gas to afford 0.50 g of *N*-{3-[(3′-fluoro-1,1′-biphenyl-4-yl)methoxy]phenyl}piperidine-4-carboxamide hydrochloride salt (**7g**), which was purified by crystallization: pale-brown crystals, 60% yield; mp 248−249 °C, from EtOH/EtOAc. ^{1}H NMR ($CDCl_3$) δ 10.11 (s, 1H), 8.87 (s, 2H), 7.71 (d, 2H, J = 8 Hz), 7.53−7.48 (m, 5H), 7.42 (d, 1H, J = 2 Hz), 7.21−7.11 (m, 3H), 6.71 (d, 1H, J = 7 Hz), 5.10 (s, 2H), 3.30 (d, 2H, J = 14 Hz), 2.88 (t, 2H, J = 14 Hz), 2.66−2.58 (m, 1H), 1.94−1.88 (m, 2H), 1.85−1.75 (m, 2H). IR (cm^{-1}) 3284, 1794, 1695, 1220, 1162, 858, 792. Anal. ($C_{25}H_{26}N_2O_2FCl$) C, H, N.

In Vitro Inhibition of Platelet Aggregation. Human blood was obtained from healthy volunteers (25−45 years of age), who had not ingested any platelet inhibitory drug for at least 1 week prior to donation. All subjects provided informed consent. Blood and blood products were handled in plastic ware, whereas siliconized glass cuvettes and stir bars were used in the aggregation assay.

Human platelet-rich plasma (PRP) was obtained from the supernatant after centrifugation of venous blood (9 mL), mixed with 0.129 mol/L sodium citrate (1:9 to blood) to prevent it from clotting, at 800 rpm for 15 min at 21 °C. Platelet-poor plasma (PPP) was obtained after centrifugation of the venous blood at 3200 rpm for 10 min. Platelet counts were adjusted to the constant value of 230000 μL^{-1} by using PPP.

Aggregation was measured by the turbidimetric method of Born, using a four-channel aggregometer (PACKS-4, Helena Laboratories S.p.A., Beaumont, TX).[43] The transmittance of PPP was taken as 100% aggregation. PRP (250 μL) was preincubated with the test compounds (5 μL solutions; final concentrations in the PRP solutions ranging from 10 μM to 1 mM) or with controls (to eliminate the effect of the solvent on the aggregation and release reaction of platelets, the final concentration of DMSO was fixed at 0.5%, v/v) at 37 °C for 5 min, during which the suspension was stirred at 800 rpm. Then, 50 μL of plasma isotonic solution (0.9%, w/v, NaCl) containing adenosine 5′-diphosphate (ADP) or epinephrine (EPN) was added to the stirred sample (10 μM final concentration), and the change in transmittance at 640 nm was recorded for 5 min. The control cuvette containing the vehicle-treated PRP followed the same sequence of events. The above concentrations of ADP and EPN proved to elicit a full response in all our PRP aggregation assays.

All the aggregation experiments were completed within 3 h from the blood collection, whereas each series of data for concentration−response curves in duplicate was collected within 1 h. Inhibition of aggregation was expressed as a percent difference of the maximum aggregatory response, and IC_{50} values (i.e., the concentration effecting 50% inhibition of aggregation), obtained by nonlinear (sigmoid) regression of aggregation inhibition (% A.I.) on log concentration of test compounds ($r^2 > 0.80$), were reported as means ± SEM of at least three different determinations.

Inhibition Assays of Factor Xa and Related Serine Proteases. The target compounds were assessed for their inhibitory activity toward factor Xa (fXa), thrombin (fIIa), and α- chymotrypsin (α-CT) by kinetic analysis using chromogenic substrates monitored at 405 nm. All buffer salts were obtained from Sigma-Aldrich Co. (Milan, Italy). Enzymes and substrates were obtained as follows: for fXa kinetic studies, 2 nM human factor Xa and 0.04 mM S-2765 (*Z*-D-Arg-Gly-Arg-*p*-nitroanilide) from Chromogenix AB-Instrumentation Laboratories (Milan, Italy); for fIIa kinetic studies, 0.41 U/mL bovine thrombin from Sigma-Aldrich (Milan, Italy) and 0.050 mM S-2238 (D-Phe-Pip-Arg-*p*-nitroanilide) from Chromogenix AB-Instrumentation Laboratories (Milan, Italy); for α-CT kinetic studies,

0.4 μg/mL bovine α-chymotrypsin and 0.185 mM *N*-succinyl-Ala-Ala-Pro-Phe-*p*-nitroanilide from Sigma-Aldrich (Milan, Italy).

In kinetic studies with fXa or fIIa, 500 μL of the enzyme solution in a 10 mM Tris buffer (pH 8), containing 0.15 M NaCl and 0.1% of PEG 6000, was mixed with 10 μL of solution of the test compound, its final concentration ranging from 10 nM to 0.25 mM; DMSO, derived from inhibitory compound stock solution, did not exceed a final concentration of 2% v/v (10 μL of DMSO in control assays). The enzymes were incubated with the test compound or its solvent (DMSO) for 30 min at 25 °C, and the reactions were initiated by the addition of 500 μL of the appropriate substrate solution in buffer. Increase in absorbance due to proteolytic cleavage of the substrate was monitored at 25 °C and 405 nm for 5 min.

In kinetic studies with α-CT, 845 μL of 50 mM Tris buffer (pH 7.5), containing 50 mM of $CaCl_2$, were added to 50 μL of enzyme solution in buffer and 5 μL of solution of the test compound (final concentration ranging from 10 nM to 0.25 mM) or its solvent (DMSO). After 10 min of incubation at 25 °C, 100 μL of the substrate solution in buffer was added and the absorbance increase at 405 nm was monitored at 25 °C for 5 min.

Initial velocities were determined by analysis of the initial linear portion of the kinetic curve, and values were plotted against log inhibitor concentration. IC_{50} values were obtained by nonlinear (sigmoid) regression calculation on dose−response plots in at least three different determinations, and used in the Cheng−Prusoff equation for calculating inhibition constants (K_i).[53]

In Vitro Coagulation Assays. Commercially available pooled lyophilized human plasma (100 μL), aPTT reagent (100 μL) and 0.025 mol/L $CaCl_2$ (100 μL) (Futura System s.r.l., Formello, Rome, Italy) were used to determine the concentration of the test compound required for doubling the activated partial thromboplastin time (aPTT). Increasing concentration of the inhibitor or solvent were added to plasma and incubated for 3 min at 37 °C. Clotting times (seconds) were determined in a coagulometer (Behnk Elektronik GmbH, Norderstedt, Germany) and compared with those from the appropriate human control plasma. Each measurement was performed in triplicate, and concentrations of the test compound which caused a 2-fold prolongation of aPTT (2 × aPTT) were calculated from concentration−response curves.

Determination of Lipophilicity Parameters by RP-HPLC. Polycratic capacity factors (log k'_w) were determined according to a previously reported RP-HPLC method.[33b,44] Compounds, dissolved in MeOH (1 mg/mL), were injected onto a Gemini C18 column (150 mm × 4.6 mm i.d., 5 μm particles) from Phenomenex Italia Srl (Castel Maggiore, Bologna, Italy) and retention data measured at regular increments of the volume fraction of methanol in 40 mM ammonium acetate aqueous solution (pH 5.0). All the measurements were made at temperature of 25 ± 1 °C, flow-rate of 1.0 mL/min and at 254 nm wavelength, on a Waters HPLC 1525 multisolvent delivery system, equipped with a Waters 2487 variable wavelength UV detector (Waters Assoc., Milford, MA). Capacity factors (k') of each compound at different mobile phase compositions (0.05 increments of MeOH volume fraction, ranging between 0.80 and 0.40) were calculated as: $k' = (t_R - t_0)/t_0$, where t_R is the retention time of the solute and t_0 is the column dead time, measured as the elution time of MeOH. In all the cases, the log k' values increased linearly with decreasing MeOH volume fraction. Linear regression analysis ($r^2 > 0.97$) was performed on at least five data points and the linear relationship extrapolated to 100% aqueous mobile phase to yield log k'_w values.

The experimental lipophilicity parameters log k'_w resulted reasonably correlated with the 1-octanol/water partition coefficients calculated with the Bio-Loom software (clogP):[54]

$$\log k'_w = 1.05\ (\pm 0.11)\ \text{clogP} - 0.33\ (\pm 0.45)$$
$$n = 28\ r^2 = 0.7891\ s = 0.5798\ F = 97.27$$

Docking Studies. The molecular models of **7d**, **7g**, **7m**, and **7p**, in their protonated forms, were built with the QXP editor and minimized using the default protocol (300 iterations, energy cutoff of 0.1 kJ·mol^{-1}, Polak−Ribiere conjugate gradient). The ligand-free protein was kept rigid, except for the side chains of the residues lying within a distance of 4 Å from ZK-807834 in the original PDB complex (1FJS) retrieved by the Brookhaven Protein Data Bank (http://www.rcsb.org/pdb/), which were settled free to relax during the minimization of the binding complexes found by the calculation routine. Finally, oxygen atom of Ser195 was marked for indicating the binding cavity and the inhibitor added and settled as completely free to move. To allow a good sampling of the conformational space, 1000 runs of Monte Carlo search, followed by conjugate gradient minimization, were performed, and the highest-scored docking hypotheses were taken into account.

Acknowledgment. We acknowledge the financial support by the Italian Ministry for Education Universities and Research (MIUR, Rome, Italy; PRIN 2005, grant no. 2005064838-002).

Supporting Information Available: Physicochemical data, IR and NMR spectra, and elemental analyses (C, H, N) of the intermediates and target compounds (**3e**, **4e**, **5a**, **5c**−**e**, **6b**, **6d**, **7a**−**c**, **7e**−**p**, **8d**). This material is available free of charge via the Internet at http://pubs.acs.org.

References

(1) Mackman, N. Triggers, targets and treatment for thrombosis. *Nature* **2008**, *451*, 914–918.
(2) (a) World Health Organization. *Atlas of Heart Disease and Stroke*; World Health Organization: Geneva, Switzerland, 2004. (b) American Heart Association. *Heart Disease and Stroke Statistics: 2008 Update*; American Heart Association: Dallas, TX, 2008.
(3) Meadows, T. A.; Bhatt, D. L. Clinical aspects of platelet inhibitors and thrombus formation. *Circ. Res.* **2007**, *100*, 1261–1275.
(4) Gresele, P.; Agnelli, G. Novel approaches to the treatment of thrombosis. *Trends Pharmacol. Sci.* **2002**, *23*, 25–32.
(5) Weitz, J. I.; Linkins, L. A. Beyond heparin and warfarin: the new generation of anticoagulants. *Expert Opin. Invest. Drugs* **2007**, *16*, 271–282.
(6) Vacca, J. P. New advances in the discovery of thrombin and factor Xa inhibitors. *Curr. Opin. Chem. Biol.* **2000**, *4*, 394–400.
(7) Stormoken, H. In *Platelets Responses and Metabolism*; Holmsen, H., Ed.; CRS Press: Boca Raton, FL, 1986; Vol. 3.
(8) Fuster, V.; Badimon, L.; Badimon, J. J.; Chesebro, J. H. The pathogenesis of coronary artery disease and the acute coronary syndromes. *N. Engl. J. Med.* **1992**, *326*, 242–250.
(9) Weksler, B. B. Antiplatelet agents in stroke prevention. Combination therapy: present and future. *Cerebrovasc. Dis.* **2000**, *10* (Suppl. 5), 41–48.
(10) Brass, L. Molecular basis for platelet activation. In *Hematology: Basic Principles and Practice* Hoffman, R., Benz, E. J., Shattil, S. J., Furie, B., Cohen, H. J., Silberstein, L. E., Eds.; Churchill Livingstone: New York, 1995; pp 1536−1552.
(11) Gachet, C. The platelet P2 receptors as molecular targets for old and new antiplatelet drugs. *Pharmacol. Ther.* **2005**, *108*, 180–192.
(12) Andronati, S. A.; Karaseva, T. L.; Krysko, A. A. Peptidomimetics−Antagonists of the Fibrinogen Receptor: Molecular Design, Structures, Properties and Therapeutic Applications. *Curr. Med. Chem.* **2004**, *11*, 1183–1211.
(13) Chackalamannil, S.; Wang, Y.; Greenlee, W. IJ.; Hu, Z.; Xia, Y.; Ahn, H.-S.; Boykow, G.; Hsieh, Y.; Palamanda, J.; Agans-Fantuzzi, J.; Kurowski, S.; Graziano, M.; Chintala, M. Discovery of a novel, orally active himbacine-based thombin receptor antagonist (SCH 530348) with potent antiplatelet activity. *J. Med. Chem.* **2008**, *51*, 3061–3064.
(14) Savi, P.; Herbert, G. M. Clopidogrel and ticlopidine: P2Y12 adenosine diphosphate antagonists for the prevention of atherothrombosis. *Semin. Thromb. Hemostasis* **2005**, *31*, 174–183.
(15) Arepally, G. M.; Ortel, T. L. Heparin-induced trombocitopenia. *N. Engl. J. Med.* **2006**, *355*, 809–817.
(16) Chan, Y. C.; Valenti, D.; Mansfield, A. O.; Stansby, G. Warfarin induced skin necrosis. *Br. J. Surg.* **2000**, *87*, 266–272.
(17) Krynetskly, E. Building individualized medicine: prevention of adverse reactions to warfarin therapy. *J. Pharmacol. Exp. Ther.* **2007**, *322*, 427–434.
(18) Hirsch, J. Current anticoagulant therapy−unmet clinical needs. *Thromb. Res.* **2003**, *109*, S1−S8.
(19) Steinmettzer, T.; Stürzebecher, J. Progress in the development of synthetic thrombin inhibitors as new orally active anticoagulants. *Curr. Med. Chem.* **2004**, *11*, 2297–2321.
(20) Gould, W. R. Recent advances in the discovery and development of direct coagulation Factor Xa inhibitors. *Curr. Pharm. Des.* **2003**, *9*, 2337–2347.

(21) Hauel, N. H.; Nar, H.; Priepke, H.; Stassen, J.-M.; Wienen, W. Structure-based design of novel potent nonpeptide thrombin inhibitors. *J. Med. Chem.* **2002**, *45*, 1757–1766.
(22) Eriksson, B. I.; Dahl, O. E.; Rosencher, N.; Kurth, A. A.; van Dijk, C. N.; Frostick, S. P.; Prins, M. H.; Hettiarachchi, R.; Hantel, S.; Schnee, J.; Büller, H. R. Dabigatran etexilate versus enoxaparin for prevention of venous thromboembolism after total hip replacement: a randomized, double-blind, noninferiority trial. *Lancet* **2007**, *370*, 949–956.
(23) Roherig, S.; Straub, A.; Pohlmann, J.; Lampe, T.; Pernerstorfer, J.; Schlemmer, K.-H.; Reinemer, P.; Perzborn, E. Discovery of the novel antithrombotic agent 5-chloro-*N*-({(5S)-2-*oxo*-3-[4-(3-oxomorpholin-4-yl)phenyl]-1,3-oxazolidin-5-yl}methyl)thiphene-2-carboxamide (BAY 59-7939): an oral, direct factor Xa inhibitor. *J. Med. Chem.* **2005**, *48*, 5900–5908.
(24) Fisher, W. D.; Eriksson, B. I.; Bauer, K. A.; Borris, L.; Dahl, O. E.; Gent, M.; Haas, S.; Homering, M.; Huisman, M. V.; Kakkar, A. K.; Kälebo, P.; Kwong, L. M.; Misselwitz, F.; Turpie, A. G. Rivaroxaban for thromboprophylaxis after orthopaedic therapy: pooled analysis of two studies. *Thromb. Haemostasis* **2007**, *97*, 931–937.
(25) (a) Quan, M. L.; Smallheer, J. M. The race to an orally active Factor Xa inhibitor: Recent advances. *Curr. Opin. Drug Discovery Dev.* **2004**, *7*, 460–469. (b) Linkins, L.-A.; Weitz, J. I. New Anticoagulant Therapy. *Annu. Rev. Med.* **2005**, *56*, 63–77.
(26) Leadley, R. J. Coagulation factor Xa inhibition: biological background and rationale. *Curr. Top. Med. Chem.* **2001**, *1*, 151–159.
(27) Eikelboom, J. W.; Hirsh, J. Combined antiplatelet and anticoagulant therapy: clinical benefits and risks. *J. Thromb. Haemostasis* **2007**, *5* (Suppl. 1), 255–263.
(28) Pérez-Gómez, F.; Alegría, E.; Berjón, J.; Iriarte, J. A.; Zumalde, J.; Salvador, A. Comparative effects of antiplatelet anticoagulant, or combined therapy in patients with valvular and nonvalvular atrial fibrillation. A randomized multicenter study. *J. Am. Coll. Cardiol.* **2004**, *44*, 1557–1566.
(29) Prandoni, P. Links between arterial and venous disease. *J. Intern. Med.* **2007**, *262*, 341–350.
(30) Schneider, D. J.; Sobel, B. E. Conundrums in the combined use of anticoagulants and antiplatelet drugs. *Circulation* **2007**, *116*, 305–315.
(31) Anderluh, P. S.; Anderluh, M.; Ilas, J.; Mravljak, J.; Dolenc, M. S.; Stegnar, M.; Kikelj, D. Toward a novel class of antithrombotic compounds with dual function. Discovery of 1,4-benzoxazin-3(4*H*)-one derivatives possessing thrombin inhibitory and fibrinogen receptor antagonistic activities. *J. Med. Chem.* **2005**, *48*, 3110–3113.
(32) (a) Feng, Z.; Gollamudi, R.; Dillingham, E. O.; Bond, S. E.; Lyman, B. A.; Purcell, W. P.; Hill, R. J.; Korfmacher, W. A. Molecular determinants of the platelet aggregation inhibitory activity of carbamoylpiperidines. *J. Med. Chem.* **1992**, *35*, 2952–2958. (b) Zheng, X.; Salgia, S. R.; Thompson, W. B.; Dillingham, E. O.; Bond, S. E.; Feng, Z.; Prasad, K. R.; Gollamudi, R. Design and synthesis of piperidine-3-carboxamides as human platelet aggregation inhibitors. *J. Med. Chem.* **1995**, *38*, 180–188. (c) Guo, Z.; Zheng, X.; Thompson, W.; Dugdale, M.; Gollamudi, R. New carbamoylpiperidines as human platelet aggregation inhibitors. *Bioorg. Med. Chem.* **2000**, *8*, 1041–1058.
(33) (a) de Candia, M.; Summo, L.; Carrieri, A.; Altomare, C.; Nardecchia, A.; Cellamare, S.; Carotti, A. Investigation of Platelet Aggregation Inhibitory Activity by Phenyl Amides and Esters of iperidinecarboxylic Acids. *Bioorg. Med. Chem.* **2003**, *11*, 1439–1450. (b) De Marco, A.; de Candia, M.; Carotti, A.; Cellamare, S.; De Candia, E.; Altomare, C. Lipophilicity-related inhibition of blood platelet aggregation by nipecotic acid anilides. *Eur. J. Pharm. Sci.* **2004**, *22*, 153–164.
(34) McMartin, C.; Bohacek, R. S. QXP: powerful, rapid computer algorithms for structure-based drug design. *J. Comput.-Aided Mol. Des.* **1997**, *11*, 333–344.
(35) Adler, M.; Davey, D. D.; Phillips, G. B.; Kim, S. H.; Jancarik, J.; Rumennik, G.; Light, D. R.; Whitlow, M. Preparation, characterization, and the crystal structure of the inhibitor ZK-807834 (CI-1031) complexed with factor Xa. *Biochemistry* **2000**, *39*, 12534–12542.
(36) Warren, L. *The PyMOL Molecular Graphics System*; DeLano Scientific LLC, San Carlos, CA; http://www.pymol.org.
(37) Lee, Y.-K.; Parks, D. J.; Lu, T.; Thieu, T. V.; Markotan, T.; Pan, W.; McComsey, D. F.; Milkiewicz, K. L.; Crysler, C. S.; Ninan, N.; Abad, M. C.; Giardino, E. C.; Maryanoff, B. E.; Damiano, B. P.; Player, M. R. 7-Fluoroindazoles as potent and selective inhibitors of factor Xa. *J. Med. Chem.* **2008**, *51*, 282–297.
(38) Olsen, J. A.; Banner, D. W.; Seiler, P.; Obst-Sander, U.; D'Arcy, A.; Stihle, M.; Müller, K.; Diederich, F. A fluorine scan of thrombin inhibitors to map the fluorophilicity/fluorophobicity of an enzyme active site: Evidence for C-F···C═O interactions. *Angew. Chem., Int. Ed.* **2003**, *42*, 2507–2511.
(39) Mitsunobu, O. The Use of Diethyl Azodicarboxylate and Triphenylphosphine in Synthesis and Transfromation of Natural Products. *Synthesis* **1981**, 1–28.
(40) Yuste, F.; Saldana, M. Selective reduction of nitrocompounds containing *O*-benzyl groups with hydrazine and Raney nickel without debenzylation. *Tetrahedron Lett.* **1982**, *23*, 147–148.
(41) (a) Tromp, R. A.; van Ameijde, S.; Puetz, C.; Sundermann, C.; Sundermann, B.; von Kuenzel, J. K.; IJzerman, A. P. Inhibition of Nucleoside Transport by New Analogues of 4-Nitrobenzylthioinosine: Replacement of the Ribose Moiety by Substituted Benzyl Groups. *J. Med. Chem.* **2004**, *47*, 5441–5450. (b) Robinson, R. P.; Laird, E. R.; Donahue, K. M.; Lopresti-Morrow, L. L.; Mitchell, P. G.; Reese, M. R.; Reeves, L. M.; Rouch, A. I.; Stam, E. J.; Yocum, S. A. Design and synthesis of 2-*oxo*-imidazolidine-4-carboxylic acid hydroxyamides as potent matrix metalloproteinase-13 inhibitors. *Bioorg. Med. Chem. Lett.* **2001**, *11*, 1211–1213. (c) Lafrance, M.; Rowley, C. N.; Woo, T. K.; Fagnou, K. Catalytic Intermolecular Direct Arylation of Perfluorobenzenes. *J. Am. Chem. Soc.* **2006**, *128*, 8754–8756. (d) Yamasaki, N.; Imoto, T.; Muray, Y.; Hiramura, T.; Oku, T.; Sawada, K. Preparation of benzimidazole derivatives as drugs. Patent WO 9724334, 1997.
(42) Stanforth, S. P. Catalytic cross-coupling reactions in biaryl synthesis. *Tetrahedron* **1998**, *54*, 263–303.
(43) Born, G. V. R. Aggregation of blood platelets by adenosine diphosphate (ADP) and its reversal. *Nature* **1962**, *194*, 927–929.
(44) de Candia, M.; Fossa, P.; Cellamare, S.; Mosti, L.; Carotti, A.; Altomare, C. Insights into structure−activity relationships from lipophilicity profiles of pyridin-2(1*H*)-one analogs of the cardiotonic agent milrinone. *Eur. J. Pharm. Sci.* **2005**, *26*, 78–86.
(45) Kooijman, E.; Tieleman, D. P.; Testerink, C.; Munnik, T.; Rijkers, D. T. S.; Burger, K. N. J.; de Kruijff, B. An electrostatic/hydrogen bond switch as the basis for specific interaction of phosphatidic acid with proteins. *J. Biol. Chem.* **2007**, *282*, 11356–11364.
(46) Böhm, H.-J.; Banner, D.; Bendels, S.; Kansy, M.; Kuhn, B.; Müller, K.; Obst-Sander, U.; Stahl, M. Fluorine in medicinal chemistry. *ChemBioChem* **2004**, *5*, 637–643.
(47) Razgulin, A. V.; Mecozzi, S. Binding properties of aromatic carbon-bound fluorine. *J. Med. Chem.* **2006**, *49*, 7902–7906.
(48) Olsen, J. A.; Banner, D. W.; Seiler, P.; Wagner, B.; Tschopp, T.; Obst-Sander, U.; Kansy, M.; Müller, K.; Diederich, F. Fluorine interactions at the thrombin active site: protein backbone fragments H-CαC═O comprise a favorable C-F environment and interactions of C-F with electrophiles. *ChemBioChem* **2004**, *5*, 666–675.
(49) Kürschner, M.; Nielsen, K.; von Langen, J. R. G.; Schenk, W. A.; Zimmermann, U.; Sukhorukov, V. L. Effect of fluorine substitution on the interaction of lipophilic ions with the plasma membrane of mammalian cells. *Biophys. J.* **2000**, *79*, 1490–1497.
(50) Akao, A.; Sato, K.; Nonoyama, N.; Masea, T.; Yasuda, N. Highly chemoselective reduction using a Rh/C−Fe$(OAc)_2$ system: practical synthesis of functionalized indoles. *Tetrahedron Lett.* **2006**, *47*, 969–972.
(51) Leban, J.; Kralik, M.; Mies, J.; Gassen, M.; Tentschert, K.; Baumgartner, R. SAR, species specificity, and cellular activity of cyclopentene dicarboxylic acid amides as DHODH inhibitors. *Bioorg. Med. Chem. Lett.* **2005**, *15*, 4854–4857.
(52) Shah, S. T. A.; Khan, K. M.; Hussain, H.; Anwar, M. U.; Feckera, M.; Voelter, W. Cesium fluoride−celite: a solid base for efficient syntheses of aromatic esters and ethers. *Tetrahedron* **2005**, *61*, 6652–6656.
(53) Ueno, H.; Yokota, K.; Hoshi, J.; Yasue, K.; Hayashi, M.; Hase, Y.; Uchida, I.; Aisaka, K.; Katoh, S.; Cho, H. Synthesis and structure−activity relationships of novel selective factor Xa inhibitors with a tetrahydroisoquinoline ring. *J. Med. Chem.* **2005**, *48*, 3586–3604.
(54) Cheng, Y.; Prousoff, W. H. Relationship between the inhibition constant (K_i) and the concentration of inhibitor which causes 50% inhibition (IC_{50}) of an enzymatic reaction. *Biochem. Pharmacol.* **1973**, *22*, 3099–3108.
(55) *Bio-Loom for Windows*, version 1.5; BioByte Corporation: Claremont, CA.

JM801141F